



**HAL**  
open science

## Chondrocyte cell adhesion on chitosan supports using single-cell atomic force microscopy

Christian Enrique Garcia Garcia, Claude Verdier, Bernard Lardy, Frédéric Bossard, Armando Félix Soltero Martinez, Marguerite Rinaudo

► **To cite this version:**

Christian Enrique Garcia Garcia, Claude Verdier, Bernard Lardy, Frédéric Bossard, Armando Félix Soltero Martinez, et al.. Chondrocyte cell adhesion on chitosan supports using single-cell atomic force microscopy. *International Journal of Polymer Analysis and Characterization*, 2021, 27 (1), pp.71-85. 10.1080/1023666X.2021.2008135 . hal-03424529

**HAL Id: hal-03424529**

**<https://hal.science/hal-03424529>**

Submitted on 10 Nov 2021

**HAL** is a multi-disciplinary open access archive for the deposit and dissemination of scientific research documents, whether they are published or not. The documents may come from teaching and research institutions in France or abroad, or from public or private research centers.

L'archive ouverte pluridisciplinaire **HAL**, est destinée au dépôt et à la diffusion de documents scientifiques de niveau recherche, publiés ou non, émanant des établissements d'enseignement et de recherche français ou étrangers, des laboratoires publics ou privés.

# 1 Chondrocyte cell adhesion on chitosan supports using single- 2 cell Atomic Force Microscopy

3 Christian Enrique García García,<sup>\*a,b</sup> Claude Verdier,<sup>\*c</sup> Bernard Lardy,<sup>d</sup> Frédéric  
4 Bossard,<sup>b</sup> Félix Armando Soltero Martínez <sup>a</sup> and Marguerite Rinaudo <sup>e</sup>

5 <sup>a</sup> Universidad de Guadalajara, Departamento de Ingeniería Química. Blvd. M. García Barragán  
6 #1451, C.P. 44430, Guadalajara, Jalisco, México; christian-enrique.garcia-garcia@univ-  
7 grenoble-alpes.fr; jfasm@hotmail.com

8 <sup>b</sup> Univ. Grenoble Alpes, CNRS, Grenoble INP\*\*, LRP, 38000 Grenoble, France \*\*Institute of  
9 Engineering Univ. Grenoble Alpes; frederic.bossard@univ-grenoble-alpes.fr

10 <sup>c</sup> Univ. Grenoble Alpes, CNRS, LIPHY, F-38000 Grenoble, France

11 <sup>d</sup> Pôle Biologie, DBTP, Biochimie des Enzymes et des Protéines, CHU-Grenoble, 38000  
12 Grenoble, France ; blardy@chu-grenoble.fr

13 <sup>e</sup> Biomaterials Applications, 6 Rue Lesdiguières, 38000 Grenoble, France.  
14 marguerite.rinaudo38@gmail.com

15 † Corresponding Author

16 \* Claude Verdier, claude.verdier@univ-grenoble-alpes.fr,

17 Tel: +33 4 76 63 59 80

## 18 Abstract

19 In this work, functional scaffolds based on electrospun chitosan nanofibers are studied in  
20 terms of their cell adhesion response. To prove cell compatibility of this biomaterial,  
21 chondrocyte interactions are investigated using atomic force microscopy **in which a single**  
22 **cell is fixed** to the cantilever and approached to the chitosan mat for a given contact time.  
23 Then, the cantilever is retracted and cell interactions are observed. Force jumps  
24 distribution for cell detachment is described and the adhesion energy is determined  
25 comparing nanofibers mats with homogeneous films and a BSA coated surface as control.  
26 **Force adhesion on chitosan film equals 460pN slightly higher than porous fiber mat (410**  
27 **pN) indicating that more cell-substrate bonds could be formed** on a flat contact surface.  
28 The adhesion on hydrophilic chitosan surface is much larger than **on the control surface**  
29 **(210 pN) due to its** positive character and ability for H-bond stabilization.

30 **Key words:** AFM, cell adhesion, chondrocyte, electrospun chitosan substrate,  
31 detachment energy

## 32 1. Introduction

33 One of the most studied biological applications of electrospun materials consists in the  
34 replacement and regeneration of damaged human tissue. Cells are supposed to use the  
35 artificial mat as a scaffold to adhere, adapt and proliferate in order to repair the injured  
36 tissue (mainly connective tissue, articular cartilage, joints and bones) affected by common  
37 diseases such as arthritis, osteoarthritis, arthropathy, joint dysfunction or after a surgery  
38 (Changhsun et al., 2008; Yamane et al., 2005). In the case of articular cartilage disorders,  
39 surgical interventions remain the viable option since no long-term efficient

40 pharmacological treatments are proposed yet (Huang, Hu, & Athanasiou, 2016; Rai,  
41 Dilisio, Dietz, & Agrawal, 2017). These invasive treatments include the extraction of the  
42 injured tissue followed by its artificial replacement in order to disrupt the progression of  
43 the illness (Changhsun et al., 2008; Nguyen & Gu, 2016).

44 With the aim of a solution for this problematic, several approaches have been proposed  
45 in the literature concluding that research about biological properties must include the  
46 investigation of cell adhesion and compatibility with the new polymeric scaffold (Huang  
47 et al., 2016; Rai et al., 2017; Yamane et al., 2005).

48 In tissue engineering, all factors influencing the behavior of cells dealing with new tissue  
49 replacements are important. The study of cell-to-scaffold adhesion could lead to a better  
50 understanding of many biological processes, especially cell migration, differentiation and  
51 proliferation (Huang et al., 2016; Titushkin & Cho, 2006). These processes are related to  
52 the cell response to their microenvironment which includes nutriment and growth factor  
53 concentrations as well as substrate morphology (chemo-mechanical properties) (Cohen,  
54 Klein, Geiger, & Addadi, 2003; Nguyen & Gu, 2016; Varady & Grodzinsky, 2016). On  
55 this point, it has been shown that fiber mats, obtained by electrospinning, with low density  
56 and high porosity are well adapted for cell development (Soliman et al., 2011).

57 Cell adhesion is the ability of a cell to stick to a surface that could be another cell, the  
58 extracellular matrix (ECM) or different scaffolds (bulk material, gels) (Puech et al.,  
59 2005). Numerous strategies and methods have been proposed and performed to quantify  
60 this interaction between cells and their environment. Laser Optical Tweezers (LOT) and  
61 Atomic Force Microscopy (AFM) are important tools for the quantification and  
62 understanding of biological sample properties at the micro and nanoscale (Changhsun et  
63 al., 2008; Iscru, Anghelina, Agarwal, & Agarwal, 2008; Nguyen & Gu, 2016; Titushkin  
64 & Cho, 2006; Ungai-Salánki et al., 2019; Whitehead, Rogers, Colligon, Wright, &  
65 Verran, 2006).

66 The AFM technique allows to characterize either normal cell-substrate interactions, cell-  
67 cell adhesion and lateral cell detachment (Nguyen & Gu, 2016). Some of the studied  
68 mechanisms to measure cell adhesion strength, applying AFM, include the approach onto  
69 an adhered cell to measure adhesion force between the cell and a functionalized cantilever  
70 tip (Changhsun et al., 2008). Measurement of adhesion force between two cells has been  
71 also performed by using cells attached to the cantilever and brought into contact with  
72 another adherent cell. Finally, AFM cantilever has been used to apply a shear force on a  
73 cell until it is detached; tangential adhesion force between the cell and the substrate is  
74 then measured (Nguyen & Gu, 2016).

75 In the particular case of chondrocytes, being related with cartilage tissue reconstruction  
76 (Changhsun et al., 2008; Nguyen & Gu, 2016), AFM helped to measure the cell response  
77 to normal and lateral external forces. AFM has also facilitated the understanding of how  
78 a disease can affect the adhesion properties and stiffness of cells. It has been reported that  
79 chondrocytes can resist normal forces better than tangential shear in the early steps of the  
80 adhesion process when adhesion molecules establish early attachment to substrates.  
81 When cells spread, strong adhesion is generated leading to higher detachment tangential  
82 shear through the formation and action of stress fiber bundles (Nguyen & Gu, 2016).

83 The method known as single-cell force spectroscopy (SCFS) consists in the  
84 immobilization of a single living cell on an AFM cantilever and the measurement of the  
85 interaction forces between the cellular entity and a bio-interface, which can be a tissue,  
86 another cell or a surface (Puech et al., 2005; Ungai-Salánki et al., 2019). In SCFS, the cell  
87 attached to the cantilever is pushed until contact with the substrate or to the other cell,  
88 allowing direct measurement of cell-surface or cell-cell adhesion, respectively. Since both  
89 spatial resolution and force sensitivity are high, the AFM was the first method able to  
90 measure cell adhesion (Puech et al., 2005; Ungai-Salánki et al., 2019).

91 In many studies, experiments involving the lateral force detachment of chondrocytes  
92 using AFM were applied in order to study the adhesive force response between cells and  
93 the substrate. In these assays, high lateral force values were observed. For instance, in the  
94 case of single living chondrocytes seeded during 3, 6 and 24 hours on a Petri dish, the  
95 adhesion force increases from  $74.14 \pm 13.81 \text{ nN}$  to  $171.02 \pm 34.24 \text{ nN}$  then to  $185.48 \pm$   
96  $39.50 \text{ nN}$ , respectively (Nguyen & Gu, 2016). Other experiments on cervical carcinoma  
97 cells were performed to investigate the effect of various adsorbed proteins on polystyrene  
98 substrates usually used for cell culture. The determined adhesion forces varied from 20  
99 to 200 nN, increasing with time and temperature; higher values were observed on  
100 hydrophilic substrates compared to hydrophobic supports, as a function of the adsorbed  
101 protein content (Sagvolden, Giaever, Pettersen, & Feder, 1999). An original technique  
102 was used to measure the strong adhesion of *Caulobacter crescentus* to a solid substrate  
103 with a suction flexible glass micropipette adapted for measuring forces ranging from tens  
104 of nN to tens of  $\mu\text{N}$ . Values around  $0.59 \mu\text{N}$  were found for the detachment force (Tsang,  
105 Li, Brun, Freund, & Tang, 2006).

106 Chitosan-based materials, especially developed for biomedical applications, have  
107 attracted attention for a long time. In terms of practicality and efficiency, non-woven  
108 membranes of electrospun nanofibers are well known for their porous structures and  
109 relatively large surface area, which provide ideal materials to mimic the natural  
110 extracellular matrix (ECM) (Ribba, Parisi, D'Accorso, & Goyanes, 2014). One advantage  
111 of chitosan, a pseudo-natural polymer, is that it becomes water soluble in acidic  
112 conditions due to  $-\text{NH}_2$  protonation as soon as its degree of acetylation is lower than 0.5;  
113 then, chitosan solution processing is relatively easy. Chitosan is an interesting  
114 biodegradable and biocompatible polymer with hemostatic properties, anti-inflammatory  
115 response, antibacterial and antifungal properties often described in the literature, and is  
116 well adapted for biological applications (Sapkota & Chou, 2020; Younes & Rinaudo,  
117 2015). In addition, chitosan is stabilized by the H-bond network in the solid state,  
118 providing good mechanical properties under film or fibrous materials.

119 Chitosan scaffolds produced by electrospinning, as an approach of a developed advanced  
120 technology to improve tissue engineering, are proposed in this research work. Being a  
121 natural based polymer and considering its particular properties such as biodegradability  
122 and non-toxicity, its application is outstanding as compared to other polymers and  
123 biopolymers. Nevertheless, the degree of acetylation of chitosan samples applied for cell  
124 development must be preferentially lower than 0.13 (Amaral, Cordeiro, Sampaio, &  
125 Barbosa, 2007).

126 In order to show the effect of the electrospun chitosan mats topography on cell adhesion,  
127 force measurements at the nanoscale provided by the AFM technique have been  
128 performed using the SCFS method. Helping to demonstrate the advantage of using  
129 chitosan-based fibers to improve chondrocyte cell adhesion in tissue engineering  
130 applications, the results are compared with the adhesion response on chitosan films as  
131 well as a BSA-coated Petri dish surface.

132 Based on the hypothesis that chitosan substrates are able to supply an appropriate  
133 environment for chondrocyte adhesion, culture and phenotype maintaining, AFM  
134 measurements will help understand and validate the choice of biomaterials from this  
135 source. Single cells fixed on the cantilever interact directly with the support allowing to  
136 quantify the force and the energy needed to separate the cell from the substrate. At the  
137 same time, analogous results can be expected between the 2 studied substrate  
138 morphologies (film and fiber) even though, chitosan fiber mats are preferable  
139 biomaterials. Adhesion energy is favored by the H-bond stabilization and possible charge  
140 interaction on chitosan supports.

## 141 **2. Experimental**

### 142 **2.1 Materials**

143 The chitosan (CS) sample was from Northern cold-water shrimp, *Pandalus borealis*, from  
144 Primex Ehf (Batch TM4778, code 42010, Siglufjordur, Iceland), with a molecular weight  
145 ( $M_w$ ) around 160 kg/mol and a degree of acetylation (DA) of 0.05, determined using  $^1\text{H}$   
146 NMR. Poly (ethylene oxide) (PEO) with a molecular weight of  $1 \times 10^3$  kg/mol was used  
147 to prepare the fibrous mat. Acetic acid ( $\geq 99.7\%$ ) was used as solvent for both polymers,  
148 ethanol and  $\text{K}_2\text{CO}_3$  were purchased from Sigma-Aldrich (France). Deionized water was  
149 used to prepare the solutions. All reagents and polymers were used as received without  
150 further purification.

151 For cell culture, the C-20/A4 human chondrocyte cell line (Goldring et al., 1994) was  
152 selected and the samples were seeded in Dulbecco's Modified Eagle Medium (DMEM)  
153 supplemented with 10% v/v of fetal bovine serum (FBS) and a 1% v/v, in proportion with  
154 the total volume, penicillin/streptomycin/glutamine solution. Phosphate Buffered Saline  
155 (PBS) solution with a pH=7.4, measured in the laboratory, DMEM serum-free and 0.05%  
156 Trypsin-EDTA solution were also utilized in cell experiments. All biological reagents  
157 were purchased from Gibco Life Technologies (Paisley, UK).

### 158 **2.2 Cell culture**

159 The initial sample of chondrocytes C-20/A4 was disposed in a culture flask, 20 mL of  
160 complete DMEM were added and the sample was preserved into a cell incubator (inCu  
161 safe, Panasonic) at 37 °C and 5%  $\text{CO}_2$  constant inlet flow during few days until  
162 confluence.

163 Before AFM tests, trypsinization was used for cell detachment from culture flask; a final  
164 cell suspension was prepared in complete DMEM containing around  $1 \times 10^6$  cell/mL.

### 165 **2.3 Engineering CS scaffolds by electrospinning**

166 Chitosan nanofibers were produced by electrospinning of the CS/PEO system at 70/30  
167 (w/w) proportion related to the total polymer concentration (5% w/w). The blend was

168 prepared in 0.5 M acetic acid and the nanofibrous scaffolds were fabricated using a  
169 conventional vertical electrospinning arrangement, as described elsewhere (Garcia,  
170 Soltero Martínez, Bossard, & Rinaudo, 2018).

171 Nanofibers were collected on an aluminum foil and the so-formed-mats were left at  
172 ambient conditions to evaporate the excess of acetic acid and water, prior to further  
173 analyses.

## 174 **2.4 Preparation of Chitosan films by evaporation casting**

175 A constant amount (~1.0 gram) of a 5% w/w CS solution was placed in a Teflon mold of  
176 known volume to obtain a uniform polymer film with a thickness between 40-50  $\mu\text{m}$   
177 (measured with a *Mitutoyo Digimatic* micrometer, with precision of 0.001mm). The  
178 probes were stored at room temperature for 3 days until complete evaporation of the  
179 solvent.

## 180 **2.5 Chitosan Neutralization**

181 Spun nanofiber mats and CS casted films were weighted and cut at the desired size before  
182 being immersed in alkaline ethanol/water 70/30 v/v mixture, prepared by dissolving  
183  $\text{K}_2\text{CO}_3$  until achieving a basic pH value around 12. This step helps to neutralize the  
184 protonated chitosan amino groups when CS is dissolved in acidic conditions (Rinaudo,  
185 2006). Further, CS films and nanofiber mats were washed for 3 days, four times a day,  
186 with deionized water until pH neutralization, to remove the salt formed from chitosan  
187 solutions (potassium acetate) and  $\text{K}_2\text{CO}_3$  excess. Finally, the membranes were dried at  
188 room temperature before being used in AFM measurements.

## 189 **2.6 Substrate fixing**

190 Substrate samples, covering the majority of the circular surface ( $9.2 \text{ cm}^2$ ) of the culture  
191 Petri dish (Techno-Plastic product AG, Switzerland), were selected.

192 UV curing NOA 68, Norland Optical Adhesive 68 (Lot 319, Norland Products, INC,  
193 Cranbury, NJ, USA), was used to stick the solid substrates to the bottom part of the culture  
194 dish. Different adhesion points were created by putting a small amount of the product  
195 between the substrate and the dish; NOA 68 was left acting during 15 minutes under UV  
196 radiation before AFM tests.

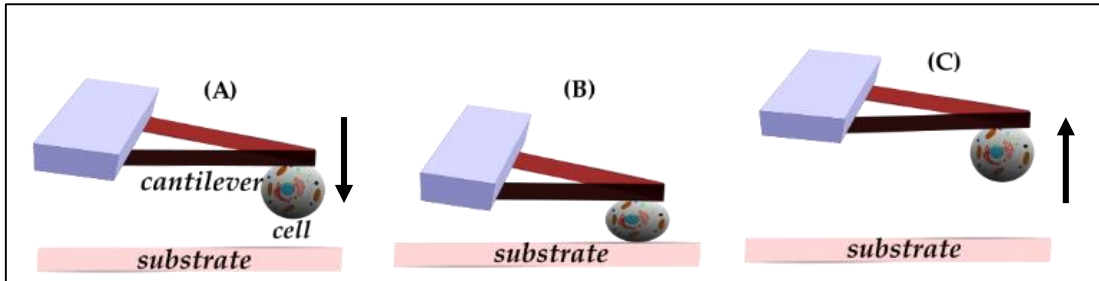
197 In order to have a reference surface for the adhesion response, a culture dish was treated  
198 with a 5mg/mL BSA solution in PBS buffer for 60 minutes. In such a case, the surface  
199 was negatively charged in the presence of the PBS buffer (pH=7.4). As culture plates are  
200 frequently treated to improve cell adhesion and spreading (Zeiger, Hinton, & Van Vliet,  
201 2013), control BSA coated surface represents a substrate where chondrocyte adhesion is  
202 partially inhibited.

## 203 **2.7 AFM Measurements**

### 204 **2.7.1 SCFS approach**

205 In AFM, a minute tip is used as a sensor, and a cantilever serves as a transducer to measure  
206 different properties, surface and force interactions between the tip and the sample by  
207 means of cantilever deflection signals. This optical signal can be converted to an electric  
208 signal by using a photodiode detector with quadrant phases and recorded on a computer.

209 When the AFM cantilever is bent by an applied force during the scanning topography or  
 210 force measurement, the angle of the deflected laser beam changes and is reflected onto  
 211 the photodiode detector. The position of the laser spot moves on the photodetector,  
 212 inducing voltaic signal changes. These signal changes can be read to quantitatively  
 213 estimate cantilever bending and force. This technique allowed the investigation of the  
 214 adhesion response of chondrocytes attached to tipless cantilevers on different chitosan  
 215 supports using normal force measurement in the process depicted in figure 1.

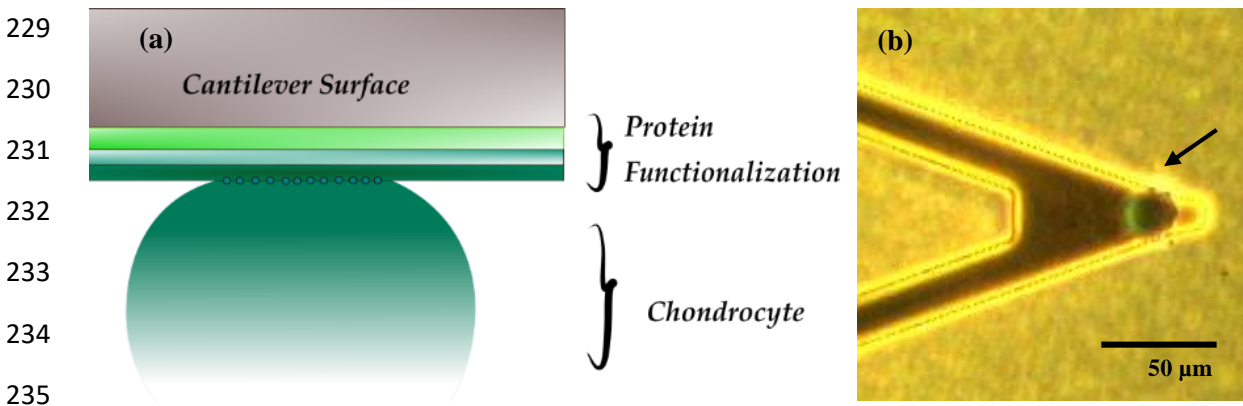


216

217 **Figure 1.** Global strategy for the cell adhesion measurements performed in this work. (A)  
 218 **Approach.** Chondrocyte is attached to the cantilever and approached to the chitosan  
 219 substrate at constant velocity. (B) **Contact.** Chondrocyte is in contact with the substrate  
 220 during the contact time ( $t_c$ ) under force ( $F_c$ ). (C) **Retraction.** The cantilever is retracted  
 221 and the cell interaction response is obtained.

222 The experiments were performed on a Nanowizard II AFM from JPK Instruments (Berlin,  
 223 Germany). Soft tipless V-shaped commercial cantilevers MLCT-O (Bruker, France) with  
 224 a spring constant ( $k$ ) around 0.01 N/m were used to measure force strength. The spring  
 225 constant was calibrated following a classical method, first the sensitivity ( $\sim 50\text{nm/V}$ ) was  
 226 found by contact on a rigid surface, then the method of thermal fluctuations (Hutter &  
 227 Bechhoefer, 1993) was used to find  $k \sim 0.01$  N/m.

228 2.7.2 Single cell binding



236 **Figure 2.** (a) Cantilever functionalization for cell attachment prior adhesion  
 237 measurements. (b) Living chondrocyte adherent to the cantilever tip (as pointed by the  
 238 black narrow) and placed on the top of chitosan film as substrate. The diameter of the  
 239 chondrocyte determined by fluorescence is around 20  $\mu\text{m}$ .

240 The global strategy consisted in the attachment of an individual chondrocyte cell, which  
 241 was extracted from its original culture medium. The cantilever was pre-treated with  
 242 different proteins allowing the binding of the cell to the cantilever tip, as it depicted in

243 figure 2a. The cantilever functionalization consisted in the use of Biotin-BSA; an  
244 overnight treatment by incubation at 37°C, followed by Streptavidin during 10 minutes  
245 under the same conditions, and the final step of the treatment involved the immersion of  
246 the tips into a Biotin-conA solution for 10 minutes (Laurent, Duperray, Sundar Rajan, &  
247 Verdier, 2014; Sundar Rajan, Laurent, Verdier, & Duperray, 2017). Intermediate  
248 cantilever rinsing with PBS between each step was carried out.

249 The chondrocyte was first captured, as shown in figure 2b, with the cantilever in 2 mL  
250 serum-free culture medium. Complete culture medium was added and the cell was then  
251 approached to the chitosan support which was fixed at the bottom part of the Petri dish.  
252 The force set point ( $F_c$ ) was selected to 0.5 nN (applied force limit in the normal direction  
253 during the contact time) and the cantilever speed was 1  $\mu\text{m/s}$ .

254 As tipless cantilevers are used for this approach, the influence of the cell on the cantilever  
255 does not change the cantilever proprieties (in particular stiffness,  $k$ ), as shown previously  
256 (Laurent et al., 2014). The most important point is that the cell should be effectively in  
257 contact with the fiber mat or chitosan film which is the case according to the force curves  
258 obtained by microscopy.

### 259 2.7.3 Analysis of AFM cell response

260 The system response to the AFM experimental procedure consists in two curves  
261 corresponding to the approach and retraction processes. Vertical force  $F(\text{nN})$  of the  
262 cantilever is represented versus piezo-height ( $z$ ). The piezoelectric device, placed at  
263 height ( $z$ )  $\sim 15 \mu\text{m}$ , moves from its position towards the bottom of the Petri dish until a  
264 vertical deflection according to the setpoint is observed. Once the contact time is  
265 achieved, the piezo retracts until the cell is completely detached from the substrate.

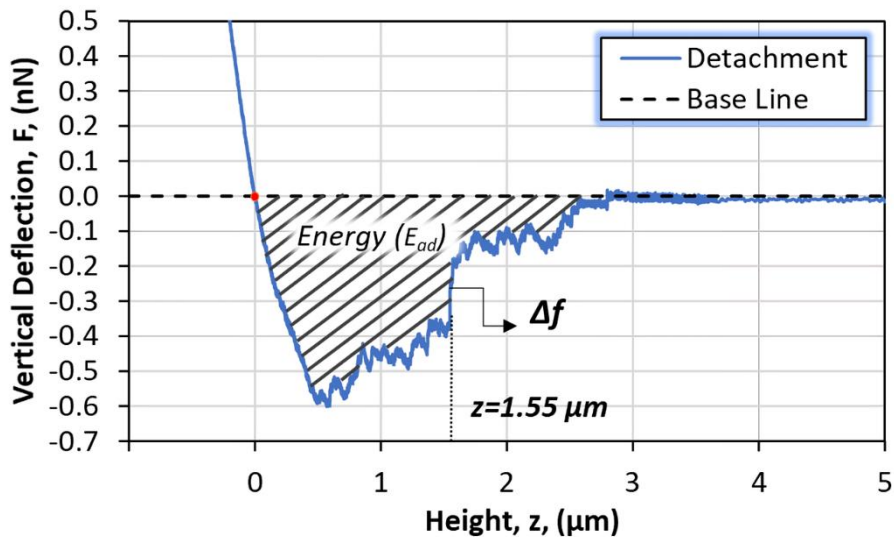
266 When the retraction region is analyzed, we are able to determine the number of significant  
267 adhesion events and the forces required to break each adhesion bond. This response **could**  
268 **be** directly related to the adherent protein distribution (**a large family of integrins and**  
269 **CD44 receptors**) among the cellular membrane that, especially in chondrocytes, mediate  
270 **the capacity of the cell to have specific interactions with the ECM and regulate cartilage**  
271 **structure (Changhsun et al., 2008). Y a-t-il des protéines spécifiques? OUI, Mais les**  
272 **molécules d'adhésion sont sélectives. Les intégrines pour le collagène et le CD44 est un**  
273 **récepteur de HA. Et pour le chitosane ????**

274 Each event, representing cell-substrate bond detachments, has a relative position ( $z$ ) and  
275 intensity ( $\Delta f$ ). Figure 3 gives an example of a detachment step location (also called force  
276 jump),  $\Delta f \sim 70 \text{ pN}$ , at  $z = 1.55 \mu\text{m}$  on the retraction curve.

277

278





279

280 **Figure 3.** Retraction curve analysis. Force jump location ( $z$ ) and intensity ( $\Delta f$ ) for  
 281 adhesion test of chondrocytes on chitosan supports. Adhesion Energy (shaded area)  
 282 represented as the integration of force ( $f$ ) vs. cantilever displacement ( $z$ ) for the  
 283 detachment response of chondrocytes on the chitosan film. Contact time = 60 s.

284 Another important aspect helping to characterize the interaction of chondrocytes to  
 285 artificial scaffolds is the adhesion energy ( $E_{ad}$ ). The adhesion energy represents the  
 286 detachment work done by the cantilever to completely detach the cell from the substrate.  
 287 This parameter involves the whole cell contact area and is derived through integration of  
 288 the area under the force (nN) curve as a function of displacement ( $z$ ), presented in figure  
 289 3. In the same context as the other parameters studied, the base line is chosen as the final  
 290 limiting value, where all bonds are considered detached (Laurent et al., 2014).

291 Tests were carried out at two different contact times (60 and 120 seconds) and two  
 292 chitosan substrates (a casted film as model and an electrospun nanofiber mat with an  
 293 average fiber diameter around 100-250 nm) (Garcia et al., 2018). A reference surface was  
 294 prepared by coating the plastic of the Petri dish with BSA. It was determined that, under  
 295 the same buffer conditions, zeta-potential indicates that cells are negatively charged.

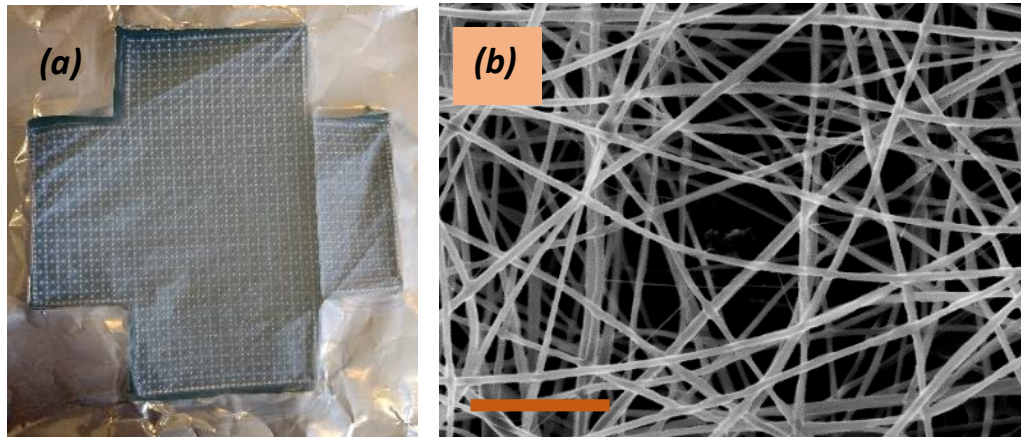
## 296 **2.8 Statistical Analysis**

297 Data for adhesion assays were generated at three independent experiments, using around  
 298 15 contact points on each sample. All results are reported as mean with standard error of  
 299 the mean (mean  $\pm$  SE) as the error bar. The value  $p < 0.01$  was considered statistically  
 300 significant for comparison between sample groups, and it was obtained by one-way  
 301 analysis of variance (ANOVA) using Excel.

## 302 **3. Results and discussion**

### 303 **3.1 Production of electrospun chitosan substrates**

304 Optimal conditions of electrospinning allowed the manufacturing of engineered chitosan-  
 305 based fiber mats. For the electrospinning processed that was performed in the laboratory,  
 306 aluminum foils cut in cross were chosen as support to remove the mat after processing.  
 307 Fibers were observed to follow the established collector pattern as it is shown in figure 4a.



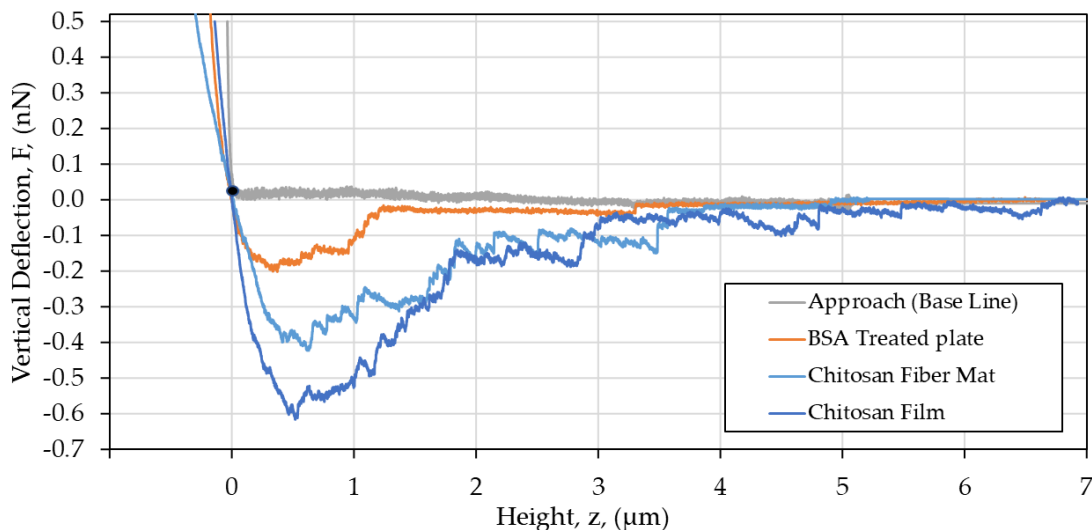
308

309 **Figure 4.** (a) Electrospun fiber mat recovered on squared-pattern collector. (b) As-spun  
 310 porous fiber mat produced from 70/30 CS/PEO solution. Scale bar = 2  $\mu\text{m}$ .

311 Morphology of electrospun chitosan fibers obtained **under the same conditions** has been  
 312 analyzed. An average diameter of  $118 \pm 36$  nm was found after diameter distribution of  
 313 the samples with a 70/30 CS/PEO proportion (Garcia et al., 2018). Smooth fibers and  
 314 homogeneous mats were observed as it is shown in figure 4b.

### 315 3.2 AFM response for force detachment

316 The contact between the chondrocyte and the surface corresponds to indentation and  
 317 adhesion interactions. After the prescribed contact time, the device retracts back, at a  
 318 velocity of 1  $\mu\text{m/s}$ , to its initial position on the vertical axis. During this step, complete  
 319 detachment of the cell occurs (in figure 5, read from left to right). In figure 5, the retraction  
 320 curve obtained on chitosan films and fiber mats are compared with the BSA coated  
 321 surface as reference.



322 **Figure 5.** Comparative response of chondrocyte detachment on chitosan substrates (film  
 323 and fiber mat) and coated Petri dish. The point (0,0) on the curve  $F$  vs  $z$  represents the  
 324 cell-substrate contact point. Retraction velocity of 1  $\mu\text{m/s}$  and data shown for a contact  
 325 time ( $t_c$ ) = 60 s.

326 Once the cell is in full contact with the substrate, the former is pushed towards the surface  
 327 until the force set point is achieved. Herein, cell indentation occurs and, depending on the

328 substrate properties, such as porosity, roughness, and swelling, a gap (in height) might be  
329 found between the approach and the retraction curves. In the same way for each material,  
330 this effect is observed in the different initial slopes on the detachment response ( $F > 0$ )  
331 (figure 5). Especially, on fiber mat with high porosity and higher water retention capacity  
332 (Garcia et al., 2018), the larger deviation (around  $-0.25 \mu\text{m}$  at  $F = 0.5 \text{ nN}$ ) was detected.

333 In all retraction curves, having a similar trend, the different steps of cell detachment are  
334 identified and they provide a complementary understanding of cell adhesion  
335 measurements. In this regard, three regions can be differentiated, including all phenomena  
336 occurring, and are proposed in figure 6.

337

338

339

340

341

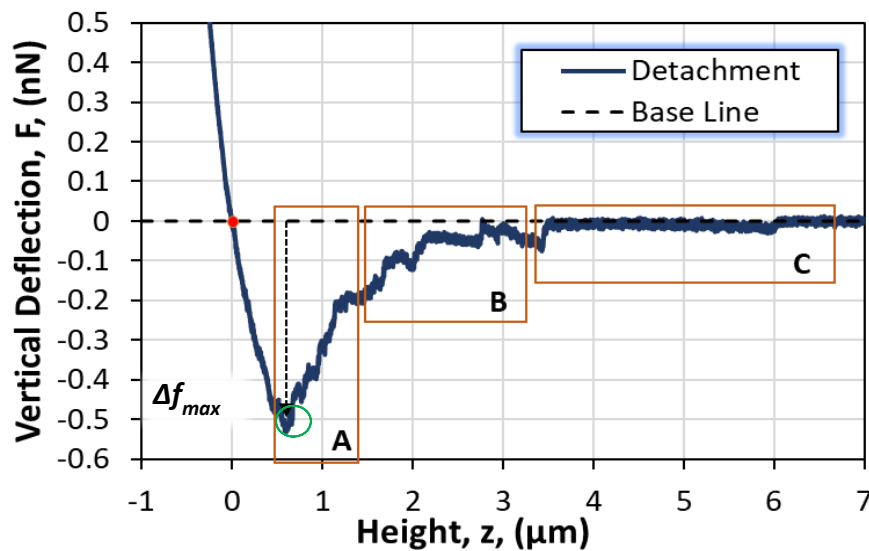
342

343

344

345

346



347 **Figure 6.** Cell detachment response separated in 3 regions or steps. Initial detachment in  
348 region A, rupture of secondary cell-substrate bonds in zone B and breaking of remaining  
349 links and return to base line in region C.

350 Included in the retraction curve, it is relevant to analyze the location and intensity of the  
351 maximum force value ( $\Delta f_{\text{max}}$ ) observed on the detachment cell response (figure 6). This  
352 value is considered as the necessary detachment force to stretch the cell and the substrate  
353 (ECM in the native tissue) until cell-substrate bonds start to break.

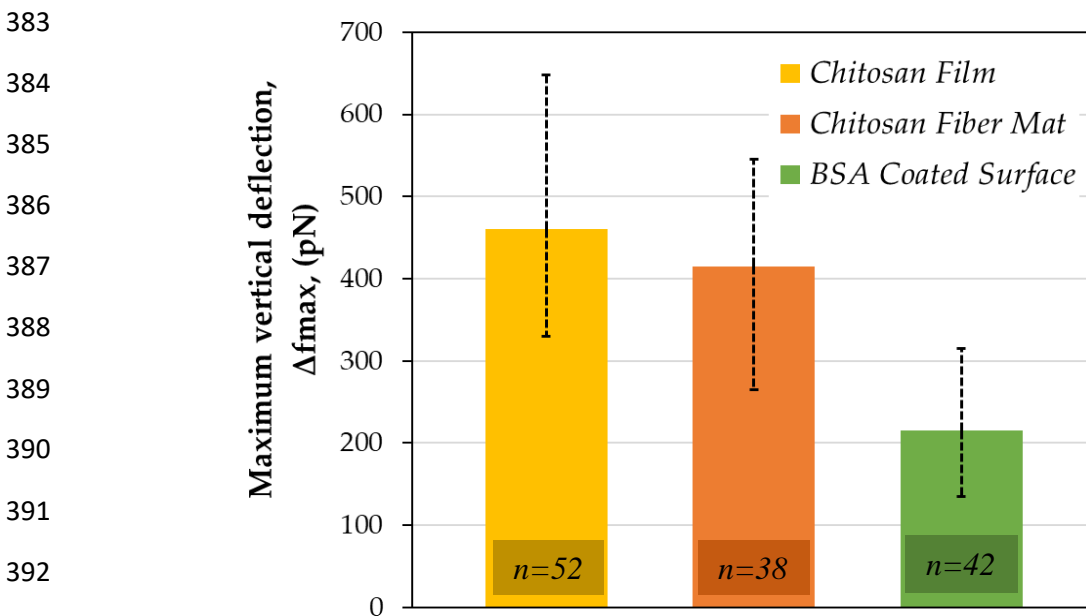
354 In zone A, the highest vertical deflection value ( $\Delta f_{\text{max}}$ ) is observed (green circle in figure  
355 6) and marks the beginning of the detachment process; this peak can be associated to the  
356 cell-substrate assembly links being stretched at the same time and the point where they  
357 start to break. In this region, more than 60% of the detected force jumps ( $\Delta f$ ) occur in the  
358 next micrometer after the first breakup, this being considered as the more representative  
359 part of the detachment response.

360 As compared to zone A, a similar phenomenon appears in region B but the normal force  
361 decreases due to the reduction of bond number between the chondrocyte and support.  
362 Finally, in region C, the final links are stretched and break as long as the cell is completely  
363 separated from the substrate surface, those links being more isolated could be associated  
364 with the individual response of cell membrane tethers (Sundar Rajan et al., 2017;  
365 Titushkin & Cho, 2006). Tether length was found between  $0.5 \mu\text{m}$  and  $1.5 \mu\text{m}$  for both

366 chitosan films and fiber mats. It is important to mention that a minority of the detected  
367 events in the retraction response take place in region C.

368 Considering all the tests performed, the maximum vertical deflection values ( $\Delta f_{\max}$ )  
369 develop in the first micrometer of the retraction step (figure 6). The distribution of these  
370 forces comparing the chitosan film and the electrospun mat for a given contact time of 60  
371 seconds is shown in figure 7. From these results, a higher maximal normal deflection  
372 ( $\Delta f_{\max}$ ) is observed when the chondrocytes interact with a more compact surface (the  
373 chitosan film) in contrast with the porous fiber mat for which the  $\Delta f_{\max}$  values are smaller  
374 and more homogenous. In the same context, significant  $\Delta f_{\max}$  differences, when  
375 comparing CS substrates from the BSA coated surface, were found for  $t_c=60$  s. This  
376 contrast between the studied substrates shows clearly that chondrocytes are around 2  
377 times more strongly adhered to CS than when they are in contact with the coated BSA  
378 culture dish.

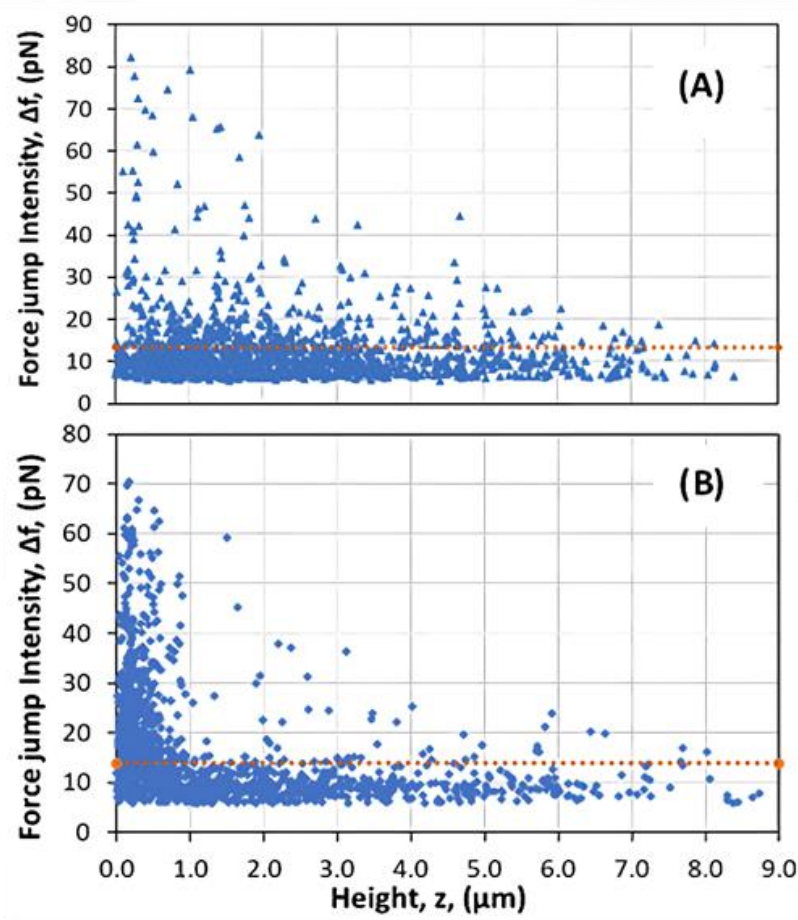
379 Average  $\Delta f_{\max}$  values between 2 and 7 nN were previously observed in adhesion tests for  
380 chondrocytes using a different AFM approach (Changhsun et al., 2008). This difference  
381 can be attributed mainly to the experimental AFM arrangement applied and the origin of  
382 the chondrocyte sample.



394 **Figure 7.** Distribution of maximum vertical force ( $\Delta f_{\max}$ ) for the two substrates studied:  
395 chitosan film and chitosan nanofibers compared to the reference BSA coated surface  
396 (significant difference found,  $p<0.01$ ), for a contact time of 60 s. Standard deviation in  
397 dotted line, number of assays = n.

398 Because the force jump intensities are coupled with a relative position on the retraction  
399 curve, the distribution of detachment steps as a function of the location on the vertical  
400 axis (separation distance) can help understand the complete adhesion phenomenon.  
401 Towards that end, registered force jumps on chitosan substrates are presented in figure 8,  
402 showing an important concentration of events during the initial part of the cell adhesion  
403 response attributed to the breakup of a large quantity of formed links and slight cell  
404 membrane deformation (zones A and B). Few force jumps are observed before complete

405 detachment of the cell, those bonds could be related to a more complex interaction  
406 between the cellular membrane and the substrates. As the cell membrane is connected to  
407 the cytoskeleton, when the former detaches, cytoskeleton filaments (membrane tethers)  
408 are also elongated few micrometers until they are released (Sundar Rajan et al., 2017;  
409 Titushkin & Cho, 2006).OK



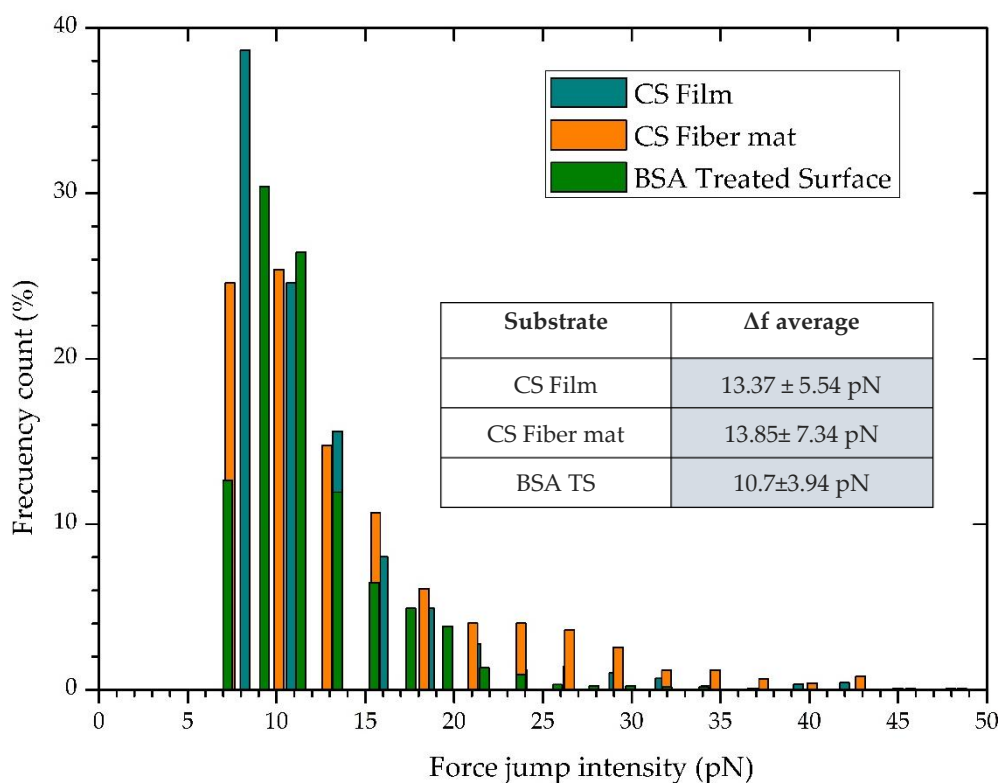
410

411 **Figure 8.** Distribution of force jumps ( $\Delta f$ ) for chondrocyte detachment from chitosan  
412 substrates vs. height ( $\mu\text{m}$ ) starting from  $\Delta f$  max. Contact time of 60 seconds on the (A)  
413 chitosan film and (B) chitosan fiber mat. Dotted lines represent the average detachment  
414 force values for the film and the fibers, 13.37 pN and 13.85 pN, respectively.

415 As shown in figure 5 and described in figure 8, force jumps are randomly located along  
416 the retraction curve. There are no specifications about the order of every detachment step  
417 but they all can be associated with the rupture, at different steps, of chondrocyte-to-  
418 substrate links formed during the pause interval when the cell membrane enters in contact  
419 with the substrate.

420 Expliquer pourquoi c'est moins disperse pour les fibres ????

421 Considering the final straight line as the base line for data analysis (figure 5), the  
422 retraction response of cells (figure 8) enables to build a frequency distribution curve of  
423 force jumps ( $\Delta f$ ), as shown in figure 9. This analysis groups in intervals all significant  $\Delta f$   
424 values, and allows to find the force jump average that could be related to an individual  
425 cell-substrate bond breaking.



426

427 **Figure 9.** Force jump distribution for cell detachment on a chitosan fiber mat for a contact  
 428 time of 60 seconds. Force jumps for CS films and the BSA coated surface are presented  
 429 in the table for a similar  $t_c$ .

430 Cell detachment force jumps ( $\Delta f$ ) for chitosan substrates were contrasted taking into  
 431 account that frequency distributions for different contact times have a similar distribution  
 432 trend. This comparison is shown in figure 8, in terms of morphology (film and fiber) as  
 433 well as in terms of affinity (BSA coated surface) for a contact time of 60 s. In the case of  
 434 a contact time of 120 seconds, there were found  $14.73 \pm 7.58$  pN and  $13.97 \pm 6.14$  pN for  
 435 CS film and fiber mat, respectively. From the obtained main values in figure 8, it is  
 436 observed that the contact time does not reflect a significant difference ( $p > 0.01$ ) on the  
 437 average detachment steps ( $\Delta f$ ) between the studied chitosan-based substrates,  
 438 independently of their morphology. This similarity could be explained for chitosan fibers  
 439 and films, since the cell type is the same in all cases and ligand-receptor interactions have  
 440 the same nature (CS-Chondrocyte).

441 It can be also remarked that the average  $\Delta f$  is higher for the chitosan films and fibers  
 442 compared to the BSA coated surface (as significant difference was found for a  $p < 0.01$   
 443 ANOVA analysis), an effect that can be attributed to the low cell-substrate selective  
 444 interaction unfavored by BSA.

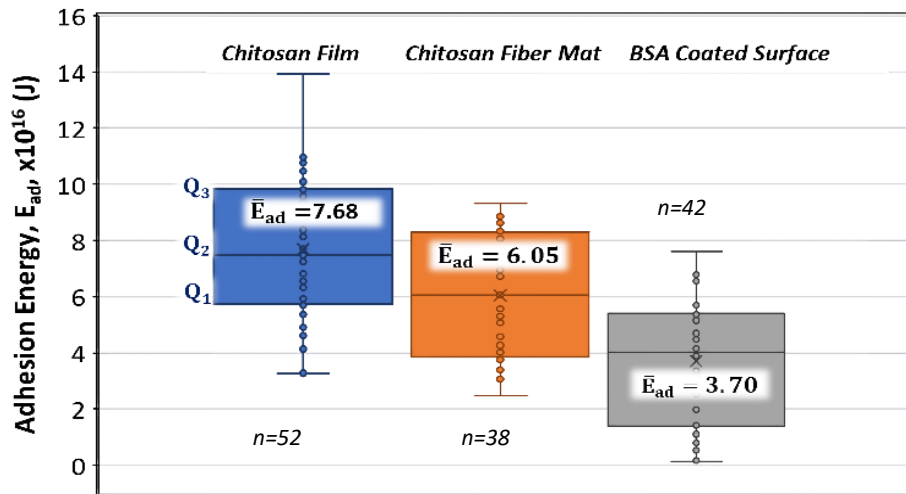
445 For the adhesion response, using the same technique for cell-cell adhesion strength,  
 446 between an endothelial cell monolayer and tumor cells, detachment steps have been  
 447 measured between 20 and 70 pN (Laurent et al., 2014; Sundar Rajan et al., 2017). These  
 448 reference values are in the same range with the obtained response in the present  
 449 experiments (detachment jumps between 10 and 80 pN in figure 7). Values acquired from  
 450 different variants of AFM methods consisting of lateral displacement or detachment from

451 a suction micropipette on different types of cells are usually larger than those obtained in  
452 this work (Sagvolden et al., 1999; Tsang et al., 2006).

### 453 3.3 Adhesion Energy of chondrocytes on chitosan substrates

454 The adhesion energy was investigated for both cell-substrate responses, the chitosan film  
455 and the fiber mat, for a contact time of 60 seconds and compared to the BSA coated  
456 surface. As shown in figure 10, this parameter was affected, as expected, by the substrate  
457 morphology. The average adhesion energy value when the chitosan film was used as  
458 chondrocyte support was found 27% higher the one observed for the nanofiber mat,  
459  $7.68 \times 10^{-16}$  J and  $6.05 \times 10^{-16}$  J, respectively. Moreover, this difference was shown to  
460 exhibit the same trend for maximum detachment force values ( $\Delta f_{\max}$ ) which are slightly  
461 higher for the chondrocyte-film interaction (see figure 9). This could be attributed to the  
462 quantity of cell-substrate bonds that were formed during the contact time and are  
463 expressed on the detachment response. On the other hand, we must consider the available  
464 contact surface when the chondrocyte touches the substrate. Due to fiber mat porosity,  
465 stiffness (Zhang, Yu, & Zhao, 2016) and morphology, a slightly smaller and softer direct  
466 area is offered for the cell to attach during the short contact with the substrate surface .

467 Furthermore, non-vertical bonds are more likely to appear on fibers than films. This  
468 phenomenon could result in a lower energy adhesion,  $\Delta f_{\max}$  values and, at the same time,  
469 affect the placement of force jumps ( $\Delta f$ ) (figure 8) on the retraction curve.



470 **Figure 10.** Adhesion Energy ( $E_{ad}$ ) distribution for AFM adhesion test on chitosan-based  
471 substrates (chitosan film and chitosan fiber mat) compared to the BSA treated surface  
472 (significant difference found,  $p < 0.01$ ). 25% of the data being lower and higher than first  
473 ( $Q_1$ ) and third ( $Q_3$ ) quartiles, respectively, are out of the box plot. The average value is  
474 represented with the cross in the colored area. Contact time equal to 60 s, number of  
475 assays = n.

476 Finally, it is important to compare the adhesion parameters on chitosan to that obtained  
477 for the surface coated with BSA (figure 4). The maximum  $\Delta f$  for chondrocytes in contact  
478 with a BSA-treated surface had a main value of  $223 \text{ pN} \pm 99 \text{ pN}$ . This response is  
479 significantly lower compared to the chitosan film and fibers ( $p < 0.01$ ). In addition, the  
480 adhesion energy value remains clearly lower than the response observed for the chitosan-  
481 based nanofiber mat and much lower than the detachment response in the case of the

482 chitosan film ( $p < 0.01$ ). The average adhesion energy determined is  $3.70 \times 10^{-16} \text{ J} \pm$   
483  $2.18 \times 10^{-16} \text{ J}$  for the BSA-treated surface.

484 The effectiveness of the BSA coating was confirmed by the application of the same AFM  
485 procedure on a culture dish utilized as bought. After force measurement, adhesion energy  
486 was found to be  $13.23 \times 10^{-16} \text{ J} \pm 3.94 \times 10^{-16} \text{ J}$ . Such a high value is expected since  
487 commercial polystyrene plates and flasks are treated to render the surfaces hydrophilic,  
488 enhancing cell–substrate adhesion (Zeiger et al., 2013).

489 From the other hand, in the buffer used, BSA coated surface is negatively charged which  
490 promotes slight electrostatic repulsion as chondrocyte membrane has also a negative  
491 character. Cell adhesion on chitosan substrates is favored due to H-bond stabilization,  
492 hydrophilicity and polarity which serves to bind proteins on its surface. Protein adsorption  
493 and subsequent cell adhesion on biomaterial surface is the essential prerequisite for  
494 biomaterial induced tissue healing (Sukul et al., 2021).

## 495 **Conclusions**

496 The cell adhesion study revealed that the adhesive response depends largely on the  
497 environmental properties of the chitosan-based materials (different morphology and  
498 surface). In this context, it was observed a slightly higher adhesion for the chitosan film  
499 compared to the chitosan fiber mat. This response can be explained considering the  
500 quantity of cell-substrate bonds that could be formed in the larger contact surface offered,  
501 in this case, by the chitosan film in contact with the cell membrane. Such bonds lead to a  
502 higher detachment force and adhesion energy values even for short contact times.  
503 Whatever the chitosan substrate used, the adhesion is favored compared to a negative  
504 BSA coated surface; a difference that involves H-bond and electrostatic loose  
505 contribution between chondrocyte and chitosan. Additionally, the porous nanofiber mat  
506 should allow cell migration, nutriment transport and permeability.

507 To our knowledge, no experimental data on SCFS have been published for chondrocytes  
508 on different CS substrates. Data from the adhesive responses presented here, allow to  
509 validate our proposed hypothesis showing that chitosan-based nanofiber mats are the  
510 most convenient supports compared with homogeneous films for chondrocyte  
511 proliferation applied in tissue engineering.

## 512 **Conflicts of interest**

513 There are no conflicts to declare.

## 514 **Author Contributions**

515 C.V., C.E.G.G. and M.R. conceived and designed the experiments; C.E.G.G. and C.V.  
516 performed the experiments; C.E.G.G., C.V., F.A.S.M., M.R., B.L. and F.B. analyzed the  
517 data and wrote the paper. All authors have read and agreed to the published version of the  
518 manuscript.

## 519 **Funding Sources**

520 This work has been financially supported by Mexican CONACYT grant 611845/788990  
521 attributed to Christian E. García García to prepare a PhD thesis in cooperation between  
522 LRP (University Grenoble-Alpes, France) and CUCEI (University of Guadalajara,



523 Mexico). We thank the Nanoscience foundation for financial support regarding the AFM  
524 platform at Liphy.

## 525 **Acknowledgements**

526 The authors acknowledge H.L. Lauzon from Primex Ehf (Iceland) for the gift of the  
527 chitosan sample and D. Roux from LRP (UGA) for his scientific interest and  
528 collaboration. LIPhy and LRP are members of the LabeX Tec 21 (Investissements  
529 d’Avenir: grant agreement No. ANR-11-LABX-0030).

## 530 **References**

531 Amaral, I. F., Cordeiro, A. L., Sampaio, P., & Barbosa, M. A. (2007). Attachment,  
532 spreading and short-term proliferation of human osteoblastic cells cultured on  
533 chitosan films with different degrees of acetylation. *Journal of Biomaterials Science,*  
534 *Polymer Edition, 18*(4), 469–485. <https://doi.org/10.1163/156856207780425068>

535 Changhsun, H., Y.-H., L., Shuming, L., Jyy-Jih, T.-W., Chung Hsiun, H. W., & Ching-  
536 Chuan, J. (2008). Surface ultrastructure and mechanical property of human  
537 chondrocyte revealed by atomic force microscopy. *Osteoarthritis and Cartilage,*  
538 *16*(4), 480–488. <https://doi.org/10.1016/j.joca.2007.08.004>

539 Cohen, M., Klein, E., Geiger, B., & Addadi, L. (2003). Organization and adhesive  
540 properties of the hyaluronan pericellular coat of chondrocytes and epithelial cells.  
541 *Biophysical Journal, 85*(3), 1996–2005. [https://doi.org/10.1016/S0006-](https://doi.org/10.1016/S0006-3495(03)74627-X)  
542 [3495\(03\)74627-X](https://doi.org/10.1016/S0006-3495(03)74627-X)

543 Garcia, C. E., Soltero Martínez, F. A., Bossard, F., & Rinaudo, M. (2018). Biomaterials  
544 based on electrospun chitosan. Relation between processing conditions and  
545 mechanical properties. *Polymers, 10*(3), 1–19.  
546 <https://doi.org/10.3390/polym10030257>

547 Goldring, M. B., Birkhead, J. R., Suen, L., Yamin, R., Mizuno, S., Glowacki, J., ...  
548 Apperleyll, J. F. (1994). Interleukin-1,8-modulated Gene Expression in  
549 Immortalized Human Chondrocytes. *J Clin Invest, 94*(6), 2307–2316.

550 Huang, B. J., Hu, J. C., & Athanasiou, K. A. (2016). Cell-based tissue engineering  
551 strategies used in the clinical repair of articular cartilage. *Biomaterials, 98,* 1–22.  
552 <https://doi.org/10.1016/j.biomaterials.2016.04.018>

553 Hutter, J. L., & Bechhoefer, J. (1993). Calibration of atomic-force microscope tips.  
554 *Review of Scientific Instruments, 64*(7), 1868–1873.  
555 <https://doi.org/10.1063/1.1143970>

556 Iscru, D. F., Anghelina, M., Agarwal, S., & Agarwal, G. (2008). Changes in surface  
557 topologies of chondrocytes subjected to mechanical forces: An AFM analysis.  
558 *Journal of Structural Biology, 162*(3), 397–403.  
559 <https://doi.org/10.1016/j.jsb.2008.02.005>

560 Laurent, V. M., Duperray, A., Sundar Rajan, V., & Verdier, C. (2014). Atomic Force  
561 Microscopy Reveals a Role for Endothelial Cell ICAM-1 Expression in Bladder  
562 Cancer Cell Adherence. *PLOS ONE, 9*(5), 1–11.  
563 <https://doi.org/10.1371/journal.pone.0098034>

564 Nguyen, T. D., & Gu, Y. (2016). Investigation of Cell-Substrate Adhesion Properties of

- 565 Living Chondrocyte by Measuring Adhesive Shear Force and Detachment Using  
566 AFM and Inverse FEA. *Scientific Reports*, 6(38059), 1–13.  
567 <https://doi.org/10.1038/srep38059>
- 568 Puech, P. H., Taubenberger, A., Ulrich, F., Krieg, M., Muller, D. J., & Heisenberg, C. P.  
569 (2005). Measuring cell adhesion forces of primary gastrulating cells from zebrafish  
570 using atomic force microscopy. *Journal of Cell Science*, 118(18), 4199–4206.  
571 <https://doi.org/10.1242/jcs.02547>
- 572 Rai, V., Dilisio, M. F., Dietz, N. E., & Agrawal, D. K. (2017). Recent strategies in  
573 cartilage repair: A systemic review of the scaffold development and tissue  
574 engineering. *Journal of Biomedical Materials Research - Part A*, 105(8), 2343–  
575 2354. <https://doi.org/10.1002/jbm.a.36087>
- 576 Ribba, L., Parisi, M., D'Accorso, N. B., & Goyanes, S. (2014). Electrospun nanofibrous  
577 mats: From vascular repair to osteointegration. *Journal of Biomedical  
578 Nanotechnology*, 10(12), 3508–3535. <https://doi.org/10.1166/jbn.2014.2046>
- 579 Rinaudo, M. (2006). Chitin and chitosan: Properties and applications. *Progress in  
580 Polymer Science (Oxford)*, 31(7), 603–632.  
581 <https://doi.org/10.1016/j.progpolymsci.2006.06.001>
- 582 Sagvolden, G., Giaever, I., Pettersen, E. O., & Feder, J. (1999). Cell adhesion force  
583 microscopy. *Proceedings of the National Academy of Sciences of the United States  
584 of America*, 96(2), 471–476. <https://doi.org/10.1073/pnas.96.2.471>
- 585 Sapkota, S., & Chou, S. (2020). Electrospun Chitosan-based Fibers for Wound Healing  
586 Applications, 4(2), 51–57. <https://doi.org/10.11648/j.jb.20200402.13>
- 587 Soliman, S., Sant, S., Nichol, J. W., Khabiry, M., Traversa, E., & Khademhosseini, A.  
588 (2011). Controlling the porosity of fibrous scaffolds by modulating the fiber  
589 diameter and packing density. *Journal of Biomedical Materials Research - Part A*,  
590 96 A(3), 566–574. <https://doi.org/10.1002/jbm.a.33010>
- 591 Sukul, M., Sahariah, P., Lauzon, H. L., Borges, J., Másson, M., Mano, J. F., ... Reseland,  
592 J. E. (2021). In vitro biological response of human osteoblasts in 3D chitosan  
593 sponges with controlled degree of deacetylation and molecular weight.  
594 *Carbohydrate Polymers*, 254(November).  
595 <https://doi.org/10.1016/j.carbpol.2020.117434>
- 596 Sundar Rajan, V., Laurent, V. M., Verdier, C., & Duperray, A. (2017). Unraveling the  
597 Receptor-Ligand Interactions between Bladder Cancer Cells and the Endothelium  
598 Using AFM. *Biophysical Journal*, 112(6), 1246–1257.  
599 <https://doi.org/10.1016/j.bpj.2017.01.033>
- 600 Titushkin, I., & Cho, M. (2006). Distinct Membrane Mechanical Properties of Human  
601 Mesenchymal Stem Cells Determined Using Laser Optical Tweezers. *Biophysical  
602 Journal*, 90(7), 2582–2591. <https://doi.org/10.1529/biophysj.105.073775>
- 603 Tsang, P. H., Li, G., Brun, Y. V., Freund, L. Ben, & Tang, J. X. (2006). Adhesion of single  
604 bacterial cells in the micronewton range. *Proceedings of the National Academy of  
605 Sciences of the United States of America*, 103(15), 5764–5768.  
606 <https://doi.org/10.1073/pnas.0601705103>
- 607 Ungai-Salánki, R., Peter, B., Gerecsei, T., Orgovan, N., Horvath, R., & Szabó, B. (2019).

- 608 A practical review on the measurement tools for cellular adhesion force. *Advances*  
609 *in Colloid and Interface Science*. <https://doi.org/10.1016/j.cis.2019.05.005>
- 610 Varady, N. H., & Grodzinsky, A. J. (2016). Osteoarthritis year in review 2015:  
611 Mechanics. *Osteoarthritis and Cartilage*, 24(1), 27–35.  
612 <https://doi.org/10.1016/j.joca.2015.08.018>
- 613 Whitehead, K. A., Rogers, D., Colligon, J., Wright, C., & Verran, J. (2006). Use of the  
614 atomic force microscope to determine the effect of substratum surface topography  
615 on the ease of bacterial removal. *Colloids and Surfaces B: Biointerfaces*, 51(1), 44–  
616 53. <https://doi.org/10.1016/j.colsurfb.2006.05.003>
- 617 Yamane, S., Iwasaki, N., Majima, T., Funakoshi, T., Masuko, T., Harada, K., ...  
618 Nishimura, S. I. (2005). Feasibility of chitosan-based hyaluronic acid hybrid  
619 biomaterial for a novel scaffold in cartilage tissue engineering. *Biomaterials*, 26(6),  
620 611–619. <https://doi.org/10.1016/j.biomaterials.2004.03.013>
- 621 Younes, I., & Rinaudo, M. (2015). Chitin and chitosan preparation from marine sources.  
622 Structure, properties and applications. *Marine Drugs*, 13(3), 1133–1174.  
623 <https://doi.org/10.3390/md13031133>
- 624 Zeiger, A. S., Hinton, B., & Van Vliet, K. J. (2013). Why the dish makes a difference:  
625 Quantitative comparison of polystyrene culture surfaces. *Acta Biomaterialia*, 9(7),  
626 7354–7361. <https://doi.org/10.1016/j.actbio.2013.02.035>
- 627 Zhang, Q., Yu, Y., & Zhao, H. (2016). The effect of matrix stiffness on biomechanical  
628 properties of chondrocytes. *Acta Biochimica et Biophysica Sinica*, 48(10), 958–965.  
629 <https://doi.org/10.1093/abbs/gmw087>
- 630